Japanese Journal of Applied Physics
Vol. 47, No. 10, 2008, pp. 8039–8042

Device Performance of the Top-Emitting Organic Light-Emitting Diodes Using the Ba/Au/Indium Tin Oxide Cathode System with Long Skin Depth

Jong Tae LIM, Chang Hyun JEONG, and Geun Young YEOM

School of Advanced Materials Science and Engineering, Sungkyunkwan University, Suwon 440-746, Korea

(Received June 17, 2008; accepted July 23, 2008; published online October 17, 2008)

This paper reports the favorable performance of a top-emitting organic light-emitting diode (TEOLED) using a Ba/Au/indium tin oxide (ITO) cathode. A cathode with a Ba layer and a long skin depth of 44.1 nm not only prevented damage to the underlying organic layers from ion bombardment during ITO sputtering, but also improved the light out-coupling of devices by increasing the transmittance. With increasing Ba thickness, the turn-on voltage and leakage current of the devices were lower than of those without Ba. The Ba layer in the cathode enhanced the optical characteristics of the devices by the balanced carrier injection. [DOI: 10.1143/JJAP.47.8039]

KEYWORDS: top-emission, organic light-emitting diode, skin depth, barium, indium tin oxide

1. Introduction

Top-emitting organic light-emitting diode (TEOLED) devices have received considerable research for use in active-matrix displays with a high aperture ratio due to their geometrical merit in allowing high pixel resolution.[1,2] TEOLEDs are expected to be useful in high-resolution full-color displays, as well as in helmet-mounted, windshield-mounted, or other head-up display applications. One of the factors that determine the device performance of TEOLED devices is the property of the top electrode, consisting of only transparent conducting oxides (TCOs) such as indium tin oxide (ITO) or semi-transparent conducting protecting layer (STCPL)/TCO.[2,4–6] The high transmittance and low resistance of the top electrode are essential for improving the device performance in terms of low driving voltage, high luminance and high efficiency. ITO thin films are used as transparent, metal-free conducting cathodes in TEOLED devices.[2] Although various methods are available for depositing ITO films, sputtering provides the benefits of high deposition rate and operating stability.[3] Furthermore, some studies have demonstrated that by facilitating a decrease in the operating voltage, sputtering offers better adhesion for the deposition of the top contact electrode than conventional thermal evaporation.[4] However, during conventional sputtering processes, the underlying organic layers can incur serious damage from the bombardment of energetic particles (such as O_2^- and O^- ions, Ar^+ ions, and γ electrons) and ultraviolet–visible (UV–vis) light.[5]

Recently, a variety of STCPLs have been developed to protect the underlying organic layers from damage during sputtering. In the STCPL/ITO cathode system, semi-transparent STCPLs, such as Ca/Ag,[6] Ag-doped Mg,[7] Al/Ag,[8] Ca,[9] and Ag,[10] have been developed. The introduction of these STCPLs improves the resistivity but decreases the transparency of the top cathode with increasing STCPL thickness. In order to increase the transmittance of an STCPL/ITO cathode, the skin depth of an individual layer composing the STCPL needs to be long. In addition, the adjoining metal layer composing the STCPL adjacent to the organic layer must have a low work function in order to improve the carrier balance by efficiently injecting an electron carrier from the cathode to the adjoining organic layer.

In this study, a Ba layer with a long skin depth was used in the STCPL for superior stability, conductivity, and optical characteristics. The Ba/Au/ITO cathode system was used to fabricate the TEOLEDs with a low operating voltage, high electroluminescence (EL) performance, and favorable protection against sputtering damage.

2. Experimental Methods

The TEOLEDs consisted of a glass/Ag (150 nm)/ITO (125 nm, about 20 Ω/□)/4,4′,4″-tris(2-naphthylphenyl-1-phenylamino)triphenylamine (2-TNATA, 30 nm)/4,4′-bis[*N*-(1-napthyl)-*N*-phenyl-amino]-biphenyl (NPB, 18 nm)/tris(8-quinolinolato)aluminium(III) (Alq_3, 62 nm)/Ba (*x* nm)/Au (5 nm)/ITO (100 nm) [$x = 15$ (device 1), 10 (device 2), 5 (device 3), 0 nm (device 4)]. All organic layers and multi-metal layer cathodes in the devices were deposited by thermal evaporation. Among the various materials composing the devices, barium is very reactive with water in air. Hence, barium was evaporated using an alkali metal dispenser (SAES Getters Alkamax) heated by a constant electrical current for a fixed period of time at a base pressure of 4×10^{-7} Torr. Meanwhile, the ITO in the multi-layer anode was deposited by conventional dc magnetron sputtering. The Ag/ITO deposited glass substrate was annealed at 350 °C for 3 min in a furnace in a nitrogen atmosphere. The ITO composing the multi-layer cathode was also deposited by dc sputtering, which was carried out at a pressure of 5 mTorr in an argon atmosphere mixed with about 0.5% oxygen and a dc power of 400 W. The ITO (refractive index: 1.95),[11] which is a transparent, index-matching layer that can enhance optical transmission, was used as the top capping layer of the TEOLED. The emissive active area of the devices was $1.4 \times 1.4\,mm^2$.

The reflectance and transmittance spectra of the electrodes were measured using a UV–vis–near infrared (NIR) spectrophotometer (Varian Cary 5000 UV/VIS/NIR) and UV spectrophotometer (SCINCO UV S-2100), respectively. The resistivity was measured using a four-point probe (CHANG MIN CMT-SERIES). The current density–voltage characteristics were measured using a source-measuring unit (Keithley 2400), and the emission intensity of the OLED devices was measured by the photocurrent induced on the silicon photodiodes using a picoammeter (Keithley 485). The luminance and external quantum efficiency were respectively calculated from the responsiveness (silicon

Table I. Skin depth at approximately 500 nm, and work function of various metals. Here, λ, E, k, δ denote the wavelength of light, photon energy, extinction coefficient in the complex index of refraction, and skin depth, respectively.

Metal	λ[15] (nm)	E[15] (eV)	k[6,14–16]	δ[6,14–16] (nm)	Work function[18] (eV)
Ba	500	2.48	0.90	44.1	2.7
Ca	500	2.48	2.00	19.9	2.9
Mg	492	2.52	2.92	13.4	3.7
Au	496	2.50	1.59	24.8	5.1
Ag	496	2.50	3.09	12.8	4.3
Al	517	2.40	6.28	6.6	4.3

photodiode) and photopic efficiency (photopic response curve) compensated for by the EL spectrum measured by optical emission spectroscopy (SC Tech. PCM-420).

3. Results and Discussion

In the TEOLED with an STCPL/ITO-type cathode, the STCPL plays an important role by protecting the underlying organic layers from bombardment during ITO deposition by sputtering, which involves the production of energetic particles such as O_2^-, O^-, and Ar^+ ions, and γ electrons. Liao *et al.* reported that at 100-eV Ar^+ irradiation, when there is no STCPL, some of the N–Al and C–O–Al bonds in the Alq_3 break, which leads to a metal-like surface acting as the leakage path.[12] Considering the energy required to break the C–C (3.73 eV), C–O (3.52 eV), C=C (6.21 eV), C–H (4.45 eV), M (e.g., Al)–O, and M–N bonds in the underlying organic layers, the energy of the energetic particles formed during conventional sputtering processes, such as the reflected Ar, reflected oxygen neutrals, and sputtered atoms, is sufficiently high (>10 eV) to break most of the bonds in the organic layers by bombardment.[13] Therefore, the individual metal layer comprising the STCPL needs to be thick enough but have sufficient transmittance to prevent bombardment damage to the underlying organic layers.

Table I shows the skin depth (δ) of various metals that have been representatively used as the STCPL. When light propagates through a metal, it can penetrate a small distance inside the metal before it is reflected. This characteristic length depends on the wavelength of incident light, and is referred to as the skin depth (δ). The δ of metals at a wavelength of approximately 500 nm was calculated as follows: $\delta = \lambda/4\pi k$ (λ: wavelength of light, k: extinction coefficient in the complex index of refraction).[6,14,15] In the case of Ba, δ was calculated from k, which was derived from the relationship between $\varepsilon_1 = n^2 - k^2$ and $\varepsilon_2 = 2nk$, where the values for ε_1 and ε_2 expressing the dielectric function ($\hat{\mathbf{e}} = \varepsilon_1 + i\varepsilon_2$) were chosen from ref. 16.

The STCPL in general has a double layer structure with a low work function, metal/oxidation-preventing metal layer. Here, a low work function metal enhances an efficiency of carrier recombination between two carriers, by improving electron injection from the cathode to electron-transporting layer (ETL). But it is not stable in air. The oxidation-preventing metal layer prevents oxidation of the low work function metal from moisture and oxygen in the air and protects the organic layers from ion bombardment damage during ITO deposition. Among the low work function metals shown in Table I, the δ of Ba (44.1 nm) was longer than that of Ca (19.9 nm)[6] and Mg (13.4 nm).[6] Moreover, Ba also exhibited the lowest work function among the metals listed. Among the oxidation-preventing metal layers, the δ of Au (24.8 nm) was longer than that of Ag (12.8 nm) and Al (6.6 nm), and it also exhibited a high chemical stability.

In this TEOLED structure, in order to increase the light-out coupling efficiency, Ag (150 nm)/ITO (125 nm) was used as a highly reflective anode (reflectance of 94% at a wavelength of 520 nm) with a low resistance (4.0×10^{-6} Ω·cm). In addition, Ba (x nm, x: 15, 10, 5, and 0)/Au (5 nm)/ITO (100 nm) with a long δ system was used as a highly transmissive cathode. During the deposition of ITO on the glass/Ag/ITO/organic layers/Ba/Au, the device can be damaged by the plasma through oxidation and physical damage of the organic layers if the thickness of the Ba/Au cathode system is inadequate. Therefore, in this study, the total thickness of the Ba/Au cathode system ranged from 5 and 20 nm in order to tune the damage to the underlying organic layers and oxidation of Ba during ITO deposition.

Figures 1(a) and 1(b) show the transmittance and reflectance spectra of the Ba (x nm)/Au (5 nm)/ITO (100 nm) cathode at wavelengths between 450 and 650 nm, respectively. The transmittance of the cathodes at wavelengths > 500 nm increased with increasing Ba thickness > 5 nm. In view of the uniform transmittance, a cathode structure with a Ba thickness of 5–15 nm showed improved flat properties of 65–72% at wavelengths of 450–650 nm, when compared with the cathode without Ba. In the case of the reflective curves shown in Fig. 1(b), for the cathodes with a Ba thickness of 5–15 nm, the reflectance was increased at wavelengths > 590 nm but decreased at wavelengths < 590 nm, compared with that of the cathode without Ba. Among the cathode structures with various Ba thicknesses, the cathode composed of Ba (15 nm)/Au (5 nm)/ITO (100 nm) showed a high transmittance of 72% and low reflectance of 15% at the maximum EL peak of 520 nm. The maximum EL peak of 520 nm in the device with a Ba (15 nm)/Au (5 nm)/ITO (100 nm) cathode was obtained by adjusting the macrocavity length,[17] which could be controlled by changing the thickness of the ITO layer composing the multilayer anode. As shown in Fig. 1, the optical properties were not insensitive to the Ba thickness variation used in this study. In addition, the high transmittance and low reflectance of the multilayer cathode were attributed to the long skin depth of both Ba and Au consisting of the STCPL. Although the mechanism for the increased transmittance and reduced reflectance induced by introducing Ba into the cathode remains to be elucidated, the change in optical properties was attributed to the difference in the interfacial geometry structure formed between Ba and Au.[18]

Figure 2 shows that increasing Ba layer thickness improved the current density–voltage characteristics of the TEOLEDs, which have a glass/Ag (150 nm)/ITO (125 nm)/2-TNATA (30 nm)/NPB (18 nm)/Alq_3 (62 nm)/Ba (x nm, x: 15, 10, 5, and 0 nm)/Au (5 nm)/ITO (100 nm) structure. The turn-on voltage, defined as the bias when the luminance is 0.1 cd/m^2, of the device with 15 nm-thick Ba was reduced by 2.4 V when compared to the device without Ba. The decrease in turn-on voltage with increasing Ba thickness suggests the formation of a stable STCPL to

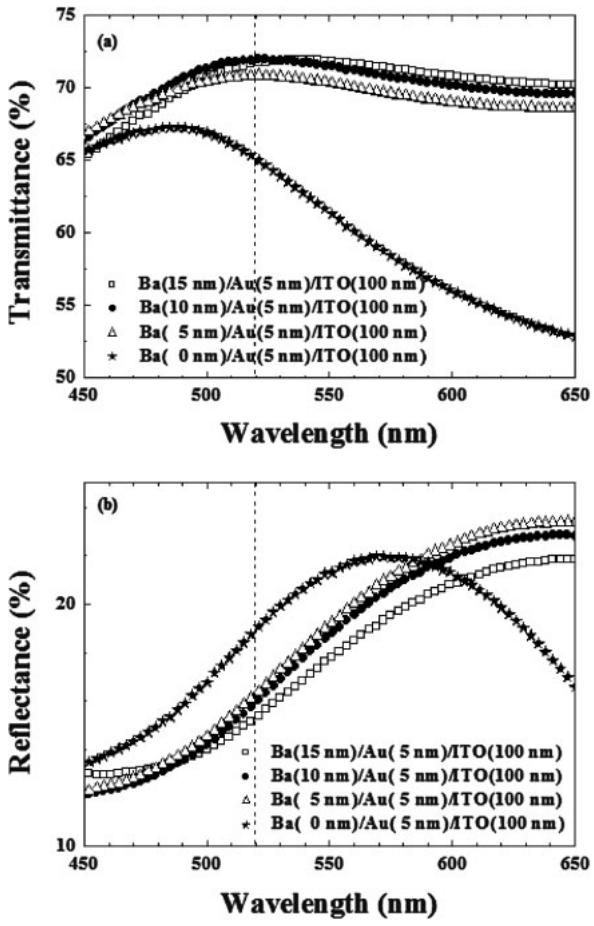

Fig. 1. (a) Transmittance and (b) reflectance spectra of Ba (*x*)/Au (5 nm)/ITO (100 nm) (*x* nm; *x*: 15, 10, 5, and 0). The broken line indicates the wavelength of electroluminescence of the emissive layer with the maximum intensity.

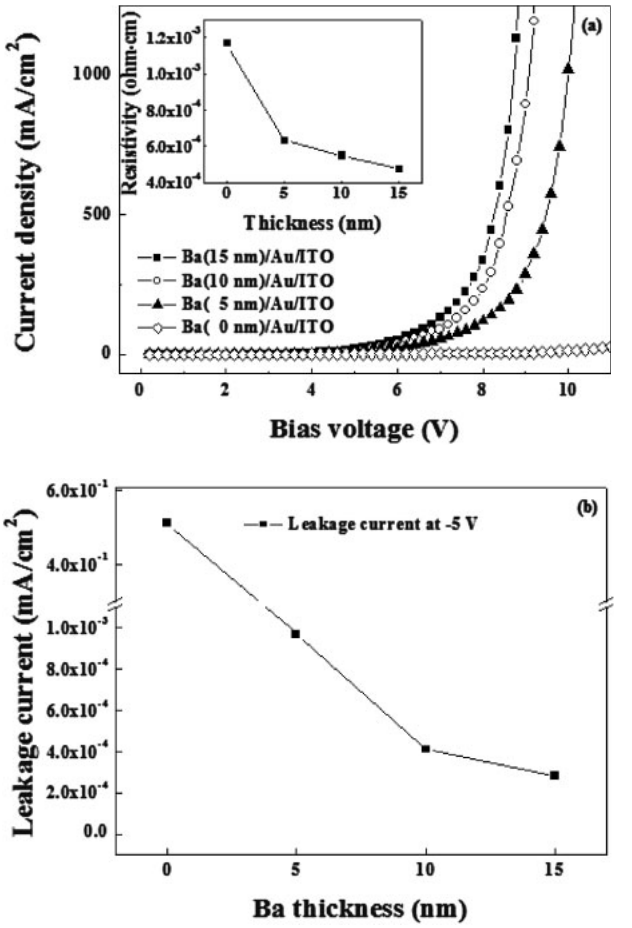

Fig. 2. (a) *J*–*V* characteristics of the TEOLD with a glass/Ag (150 nm)/ITO (125 nm)/2-TNATA (30 nm)/NPB (18 nm)/Alq_3 (62 nm)/Ba (*x* nm, *x*: 15, 10, 5, and 0 nm)/Au (5 nm)/ITO (100 nm) structure. The inset shows the resistivity of the sample structures of Si/Ba (*x* nm, *x*: 15, 10, 5, and 0)/Au (5 nm)/ITO (100 nm). (b) Leakage current variation with varying Ba thicknesses.

protect the underlying organic layers from sputtering damage. In addition, the Ba layer functions as a metal with good electrical characteristics. However, the devices with no Ba or the insertion of a Ba layer <5 nm into the cathode layer resulted exhibited poor performance due to the formation of both defects and local trap sites during ITO sputtering, which degraded the structural and electrical characteristics of the organic films.

The inset in Fig. 2(a) shows the resistivity of the Ba/Au/ITO layers on the Si wafer with increasing Ba thickness from 0 to 15 nm. The resistivity of the multilayer cathode was 11.6, 6.32, 5.48, and 4.76×10^{-4} Ω·cm at a Ba layer thickness of 0, 5, 10, and 15 nm, respectively. Therefore, the conductivity of the multilayer cathode improved almost monotonically with increasing Ba thickness in the STCPL.

Figure 2(b) shows the leakage current density at −5 V as a function of the Ba thickness from 0 to 15 nm. The leakage current densities of the devices with a Ba layer thickness of 15, 10, 5, and 0 nm were 2.8×10^{-4}, 4.1×10^{-4}, 9.7×10^{-4}, and 5.1×10^{-1} mA/cm^2, respectively. The insertion of a 5–15 nm Ba layer decreased the leakage current to three orders of magnitude lower than that of the Au/ITO cathode without Ba. The high leakage current density of the device with the Au/ITO cathode was attributed to bond breaking of the organic molecules, such as Alq_3, as a result of the bombardment effect during the ITO sputter deposition process, which causes the metal-like surface to act as a leakage path.[12] In addition, the decrease in leakage current with increasing Ba thickness from 5 to 15 nm was attributed to the decrease in plasma damage during ITO deposition.

Figure 3 shows the external quantum efficiency–luminance–power efficiency characteristics of TEOLED devices 1–4. The external quantum efficiencies (η_{ext}) for devices 1, 2, 3, and 4 were 1.9, 1.7, 1.14, and 0.2%, respectively, and the power efficiency (η_{PE}) was 3.37, 3.12, 2.32, and 0.25 lm/W, respectively. Meanwhile, the luminance (L_{max}) at a voltage of 9.4 V for devices 1, 2, 3, and 4 was 37200, 36500, 13500, and 80 cd/m^2, respectively (data not shown). Device 1, with the cathode structure of Ba (15 nm)/Au (5 nm)/ITO (100 nm), showed the best device performance considering the optical properties of the multilayer cathode and the electrical properties of the devices, such as the turn-on voltage, leakage current and efficiency. The improved light-out coupling properties of device 1 were explained by a mechanism associated with (i) protection of the underlying organic layers from bombardment damage due to a stable STCPL during the ITO sputtering process, (ii) the improved optical properties in the cathode system with the long skin depth, (iii) the low resistance of the Ba/Au/ITO cathode, and (iv) the balanced exciton recombination as a result of

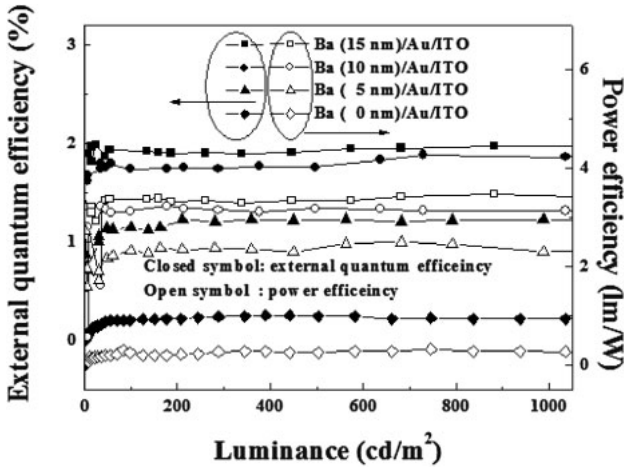

Fig. 3. External quantum efficiency–luminance–power efficiency characteristics of the TEOLED with the cathode consisting of Ba (*x* nm, *x*: 15, 10, 5, and 0 nm)/Au (5 nm)/ITO (100 nm).

efficient electron injection from the low work function cathode to the ETL.

4. Conclusions

This study demonstrated the favorable performance of TEOLEDs containing a Ba/Au/ITO cathode with a long skin depth. The cathode of Ba (15 nm)/Au (5 nm)/ITO (100 nm) showed a high transmittance of 72% and a reflectance of 15%, due to the long skin depth of Ba and Au comprising the STCPL. The insertion of a Ba layer into the cathode efficiently protected the organic emitting layer from damage caused by sputtering bombardment during deposition from the top cathode, even when the total STCPL thickness was as thin as 15 nm. In addition, the presence of the Ba layer not only facilitated electron injection but also suppressed the leakage current.

Acknowledgments

This work was supported by the National Program for Tera-Level Nano devices of the Korea Ministry of Education, Science and Technology (MEST) as a 21st Century Frontier Program.

1) V. Bulovic, G. Gu, P. E. Burrows, M. E. Thompson, and S. R. Forrest: Nature **380** (1996) 29.
2) G. Parthasarathy, P. E. Burrows, V. Khalfin, V. G. Kozlov, and S. R. Forrest: Appl. Phys. Lett. **72** (1998) 2138.
3) T. Minami: MRS Bull. **25** (2000) No. 8, 38.
4) H. Suzuki and M. Hikita: Appl. Phys. Lett. **68** (1996) 2276.
5) H. K. Kim, D. G. Kim, K. S. Lee, M. S. Huh, S. H. Jeong, K. I. Kim, and T. Y. Seong: Appl. Phys. Lett. **86** (2005) 183503.
6) R. B. Pode, C. J. Lee, D. G. Moon, and J. I. Han: Appl. Phys. Lett. **84** (2004) 4614.
7) G. Pathasarathy, C. Adachi, P. E. Burrows, and S. R. Forrest: Appl. Phys. Lett. **76** (2000) 2128.
8) C.-H. Chung, Y.-W. Ko, Y.-H. Kim, C.-Y. Sohn, H. Y. Chu, and J. H. Lee: Appl. Phys. Lett. **86** (2005) 93504.
9) M.-H. Lu, M. S. Weaver, T. X. Zhou, M. Rothman, R. C. Kwong, M. Hack, and J. J. Brown: Appl. Phys. Lett. **81** (2002) 3921.
10) K.-C. Liu, C.-W. Teng, Y.-H. Lu, J.-H. Lee, and L.-C. Chen: Electrochem. Solid-State Lett. **10** (2007) J120.
11) L. S. Hung, C. W. Tang, M. G. Mason, P. Raychudhuri, and J. Madathil: Appl. Phys. Lett. **78** (2001) 544.
12) L. S. Liao, L. S. Hung, W. C. Chan, X. M. Ding, T. K. Sham, I. Bello, C. S. Lee, and S. T. Lee: Appl. Phys. Lett. **75** (1999) 1619.
13) P. F. Carcia, R. S. McLean, M. H. Reilly, Z. G. Li, L. J. Pillione, and R. F. Messier: J. Vac. Sci. Technol. A **21** (2003) 745.
14) M. Scalora, M. J. Bloemer, A. S. Pethel, J. P. Dowling, C. M. Bowden, and A. S. Manka: J. Appl. Phys. **83** (1998) 2377.
15) D. R. Lide: *CRC Handbook Chemistry and Physics* (CRC Press, Boca Raton, FL, 2003–2004) 84th ed.
16) J. G. Endriz and W. E. Spicer: Phys. Rev. B **2** (1970) 1466.
17) G. Patharathy, C. Shen, A. Kahn, and S. R. Forrest: J. Appl. Phys. **89** (2001) 4986.
18) W. Benenson, J. W. Harris, H. Stocker, and H. Luttz: *Handbook of Physics* (AIP Press, New York, 2002).